Iron Substitution in Lithium-Overstoichiometric "$Li_{1.1}CoO_2$": Combined ^{57}Fe Mössbauer and ^{7}Li NMR Spectroscopies Studies

Michel Ménétrier,* Yang Shao-Horn,† Alain Wattiaux, Léopold Fournès, and Claude Delmas

Institut de Chimie de la Matière Condensée de Bordeaux-CNRS and Ecole Nationale Supérieure de Chimie et Physique de Bordeaux, Université Bordeaux I, 87 av. Dr A. Schweitzer, 33608 Pessac Cedex, France

Received February 25, 2005. Revised Manuscript Received May 12, 2005

Iron substitution was attempted by direct solid-state synthesis in stoichiometric $LiCoO_2$ and lithium-overstoichiometric "$Li_{1.1}CoO_2$". Iron substitution was not obtained in stoichiometric $LiCo_{0.98}Fe_{0.02}O_2$ samples, consistent with the fact that the size of Fe^{3+} ions is significantly larger than that of Co^{3+} ions in the octahedral site. In contrast, up to 8 atom % iron could be substituted in the lithium-overstoichiometric "$Li_{1.1}CoO_2$" samples with an actual composition of $Li_{1.04}Co_{0.96}O_{1.96}$, which could be rationalized by considering the structural defect model proposed previously by some of us. In the defect model, lithium-overstoichiometric samples consist of excess Li^+ replacing Co^{3+} charge-compensated by an oxygen vacancy in the cobalt layers, which creates two adjacent square-based pyramids containing intermediate-spin (IS) Co^{3+} ($[Li]_{interslab}[Co^{3+(LS)}_{1-3t}Co^{3+(IS)}_{2t}Li_t]_{slab}[O_{2-t}]$, with $t = 0.04$ and 0.08 IS Co^{3+} and LS = low spin). ^{7}Li MAS NMR showed that the signals associated with intermediate-spin Co^{3+} decreased but were not completely suppressed upon iron substitution, even for the 8 atom % Fe-substituted sample, with no new signal appearing in iron-substituted lithium-overstoichiometric samples. Moreover, the values of Mössbauer parameters, isomer shift 0.249 mm·s^{-1} and quadrupolar splitting 0.4 mm·s^{-1}, revealed that high-spin Fe^{3+} was present in the square-pyramidal sites in the 2 atom % iron-substituted lithium-overstoichiometric sample. These results lent further support for the nature of the defects proposed previously for lithium-overstoichiometric "$Li_{1.1}CoO_2$".

Introduction

$LiCoO_2$ is the most widely used positive electrode material for lithium rechargeable batteries. Its structure belongs to the trigonal system (space group $R\bar{3}m$) with a layered α-$NaFeO_2$-type framework in which cobalt and lithium layers alternate in the AB CA BC packing of the oxygen layers. This compound is prepared typically from Co_3O_4 and Li_2CO_3 at 900 °C under oxygen or in air, and its actual chemical composition depends on the Li/Co ratio of precursors used for the synthesis. As Li_2CO_3 (or Li_2O at high temperature) acts as a flux during the synthesis, it is often used in slight excess to obtain controlled-size particles suitable for use in the positive electrode of lithium batteries. This yields a lithium-overstoichiometric $LiCoO_2$ material, which has electrochemical behavior different from that of stoichiometric $LiCoO_2$ in the following two aspects: (1) the two-phase plateau found in Li_xCoO_2 with $0.75 \leq x \leq 0.94$[1−3] is reduced or suppressed completely,[4] and (2) the voltage inflection for $x \approx 0.5$ associated with lithium and vacancy ordering[5] is not present.

In previous reports,[4,6] some of us extensively discussed the structure and physical and electrochemical properties of lithium-overstoichiometric $LiCoO_2$ ("$Li_{1.1}CoO_2$"). Some key points are recalled hereafter: (1) after prolonged annealing of lithium-overstoichiometric $LiCoO_2$ at 900 °C, the excess lithium is removed in the form of Li_2O, yielding stoichiometric $LiCoO_2$, (2) even very high oxygen pressure does not suppress the defect from lithium-overstoichiometric $LiCoO_2$, and (3) it cannot be induced from stoichiometric $LiCoO_2$ by oxygen "pumping" using titanium. On the basis of these observations as well as ^{7}Li NMR, neutron and X-ray diffraction, and magnetic susceptibility data, we proposed that the excess Li^+ ions were accommodated in the cobalt sites, with the creation of an equal number of oxygen vacancies for charge compensation. This has led to the formula $[Li]_{interslab}[Co^{3+(LS)}_{1-3t}Co^{3+(IS)}_{2t}Li_t]_{slab}[O_{2-t}]$ (LS = low spin, IS = intermediate spin) for lithium-overstoichiometric samples, with t close to 0.04 in the "$Li_{1.1}CoO_2$" (1.1 being the Li/Co ratio used for the synthesis) sample prepared in the previous study,[6] which consists of an IS configuration for $2t$ Co^{3+} ions in the square-based pyramidal sites, as shown in Figure 1. In contrast to diamagnetic, LS octahedral Co^{3+}, the intermediate-spin configuration provides electron spins

* To whom correspondence should be addressed. E-mail: michel.menetrier@icmcb-bordeaux.cnrs.fr. Phone:+ 33 (0)5 56 84 66 39. Fax: + 33 (0)5 56 84 27 61.

† Present address: Department of Mechanical Engineering, Massachusetts Institute of Technology, Cambridge, MA 02139.

(1) Reimers, J. N.; Dahn, J. R. *J. Electrochem. Soc.* **1992**, *139*, 2091−2097.
(2) Ohzuku, T.; Ueda, A. *J. Electrochem. Soc.* **1994**, *141*, 2972−2977.
(3) Ménétrier, M.; Saadoune, I.; Levasseur, S.; Delmas, C. *J. Mater. Chem.* **1999**, *9*, 1135−1140.
(4) Levasseur, S.; Menetrier, M.; Suard, E.; Delmas, C. *Solid State Ionics* **2000**, *128*, 11−24.
(5) Shao-Horn, Y.; Levasseur, S.; Weill, F.; Delmas, C. *J. Electrochem. Soc.* **2003**, *150*, A366−A373.
(6) Levasseur, S.; Ménétrier, M.; Shao-Horn, Y.; Gautier, L.; Audemer, A.; Demazeau, G.; Largeteau, A.; Delmas, C. *Chem. Mater.* **2003**, *15*, 348.

10.1021/cm0504384 CCC: $30.25
Published on Web 08/13/2005

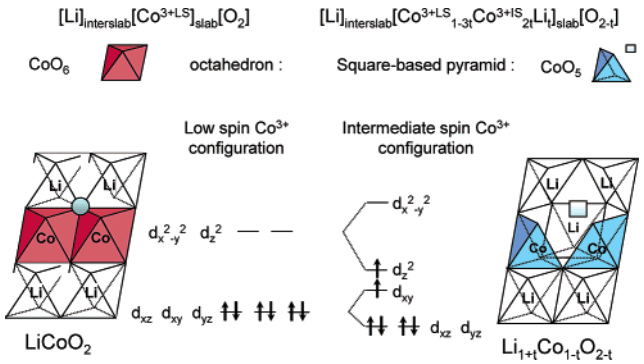

Figure 1. Schematic representation of the structural defect induced by Li^+ substitution and the resulting electronic configuration for the neighboring Co^{3+} ions.

in the d_{z^2} and d_{xy} orbits of Co^{3+}, which lead to the observed ^{7}Li NMR signals due to the Fermi contact shift interaction (transfer of some density of electron spin to the nearby Li^+ ions via orbital overlaps). Although ^{7}Li NMR, being extremely sensitive to this defect in comparison to X-ray powder diffraction that cannot discriminate between stoichiometric $LiCoO_2$ and lithium-overstoichiometric "$Li_{1.1}CoO_2$", was the starting point of these studies,[4] a complete assignment of observed NMR signals based on the proposed structural defect is yet to be achieved.

Mössbauer measurements allow the observation of interactions between the nucleus and the chemical environment. The experimentally measured isomer shift, δ, is approximated to the shift depending on the electron density at the ^{57}Fe nucleus only, which is directly proportional to the sum of the 1s, 2s, 3s, and 4s electron densities at the iron nucleus. The wave function of 3s electrons is strongly related to the 3d electron configuration and the chemical state of the iron as a result of the shielding of the 3s electrons by the 3d ones (the 3d wave function has a radial component closer to the nucleus than that of the 3s wave function, and the effective 3s electronic charge interacting with the nucleus is thus reduced by electrons in the 3d orbital). In the case of ^{57}Fe, the isomer shift decreases with increasing electron density on the nucleus. It has been shown that the isomer shift decreases with increasing oxidation states of iron and reduced coordination of iron.[7] In the proposed structural defect model for lithium-overstoichiometric "$Li_{1.1}CoO_2$", MO_5 coordination in the square-based pyramidal sites[8] will potentially lead to lower isomer shifts for $^{57}Fe^{3+}$ than octahedral FeO_6 sites. In this study, we explore ^{57}Fe substitution in stoichiometric $LiCoO_2$ (leading to $LiCo_{1-x}Fe_xO_2$) and lithium-overstoichiometric "$Li_{1.1}CoO_2$" samples (leading to $Li_{1.04}Co_{0.96-x}Fe_xO_{1.96}$) and compare the chemical environments of $^{57}Fe^{3+}$ in these samples by combined ^{57}Fe Mössbauer and ^{7}Li NMR spectroscopies in attempts to gain further insight into the nature of the defects found in lithium-overstoichiometric $LiCoO_2$.

Experimental Section

Samples with nominal compositions of "$LiCo_{0.98}Fe_{0.02}O_2$" and "$Li_{1.1}Co_{1-x}Fe_xO_2$" (actually $Li_{1.04}Co_{0.96-x}Fe_xO_{1.96}$) with $0 \le x \le 0.1$ were prepared by heat-treating a mixture of Li_2CO_3, Fe_2O_3, and Co_3O_4 (decomposition at 450 °C under oxygen of $Co(NO_3)_2 \cdot 6H_2O$ from Fluka, containing less than 0.05% Ni and 0.005% Fe) with a starting Li/Co ratio of 1.0 or 1.10 and an appropriate ratio of Fe to Co under atmospheric O_2 flow at 600 °C for 12 h with one subsequent treatment at 900 °C for 24 h. In addition, ^{57}Fe-enriched samples with nominal compositions of "$Li_{1.1}Co_{0.98}{}^{57}Fe_{0.02}O_2$" and "$Li_{1.1}Co_{0.94}{}^{57}Fe_{0.06}O_2$" were synthesized using $^{57}Fe_2O_3$ according to the same procedure as described above.

X-ray diffraction patterns of $LiCo_{0.98}Fe_{0.02}O_2$ and "$Li_{1.1}Co_{1-x}Fe_xO_2$" with $0 \le x \le 0.1$ samples were collected using a Siemens D5000 powder diffractometer with Cu Kα radiation and a graphite-diffracted beam monochromator. Data were collected at a step size of 0.02° (2θ) and step times of 20−40 s in the range of 10−100° (2θ). To detect trace impurity phases—such as α-$LiFeO_2$, Fe_3O_4, Co_3O_4, and Li_2CO_3, X-ray diffraction patterns were also systematically recorded using an INEL CPS120 diffractometer in a Debye−Scherrer configuration with Co Kα radiation or a PANalytical X'Pert Pro diffractometer in a reflection geometry equipped with a fast X'Celerator detector using Co Kα radiation.

^{7}Li MAS NMR spectra were recorded on a Bruker Avance 500 spectrometer at 193.7 MHz, with a standard 4 mm Bruker MAS probe. The samples were mixed with dry silica (typically 50% in weight), to facilitate the spinning and improve the field homogeneity, and the mixture was introduced into a 4 mm zirconia rotor. A Hahn echo sequence $[t_{\pi/2}-\tau_1-t_\pi-\tau_2]$ was utilized to facilitate the phasing of all the signals and their spinning sidebands and to ensure the observation of very wide signals due to hyperfine dipolar interactions, which would be otherwise lost during the receiver dead time in single-pulse experiments. The 90° pulse duration used ($t_{\pi/2}$) was equal to 2.1 μs, and the spinning speed (ν_r) was 15 kHz. To synchronize the spin−echo with the first rotational echo, τ_1 was fixed to the rotor period $T_r = 1/\nu_r$. A spectral width of 500 kHz was used, and the recycle time $D_0 = 2$ s was checked to be long enough to avoid T_1 saturation effects. The isotropic shifts reported in parts per million are relative to the peak for an external sample of 1 M LiCl aqueous solution.

Mössbauer measurements were performed using a constant-acceleration HALDER-type spectrometer with a room temperature ^{57}Co source (Rh matrix) in transmission geometry. The polycrystalline absorbers containing about 0.2 mg·cm^{-2} ^{57}Fe were used to avoid the experimental widening of the peaks. The velocity was calibrated using pure iron metal as the standard material. Powder samples were pressed onto an aluminum foil, and measurements were collected in an airtight holder with Mylar windows at room temperature. The Mössbauer spectra were refined in two steps. In the first treatment, Lorentzian peaks were assumed and the position (isomer shift, δ), amplitude, and width of each peak were refined. This preliminary calculation allowed the determination of experimental hyperfine parameters for the various iron sites present in the oxide. The second computation allowed the analysis of spectra in terms of quadrupolar splitting distribution $P(\Delta)$ using the method of Hesse et al.[9] This method is often used for disordered compounds with a distribution of different environments, which gives rise to strong line broadening and to line shapes differing from those of a Lorentzian profile. In the second treatment, the half-height width Γ was fixed at 0.35 mm·s^{-1} and the isomer shifts were fixed at values determined in the first treatment.

Results and Discussion

X-ray Powder Diffraction Analysis. X-ray powder diffraction patterns of "$LiCo_{0.98}Fe_{0.02}O_2$", "$Li_{1.1}Co_{0.98}{}^{57}Fe_{0.02}O_2$",

(7) Menil, F. *J. Phys. Chem. Solids* **1985**, *46*, 763−786.
(8) Long, G. J. In *Mossbauer spectroscopy*; Dickson, D. P. E., Berry, F. J., Eds.; Cambridge University Press: Cambridge, U.K., 1986; p 121.
(9) Hesse, J.; Rubartsch, A. *J. Phys. E: Sci. Instrum.* **1974**, *7*, 526.

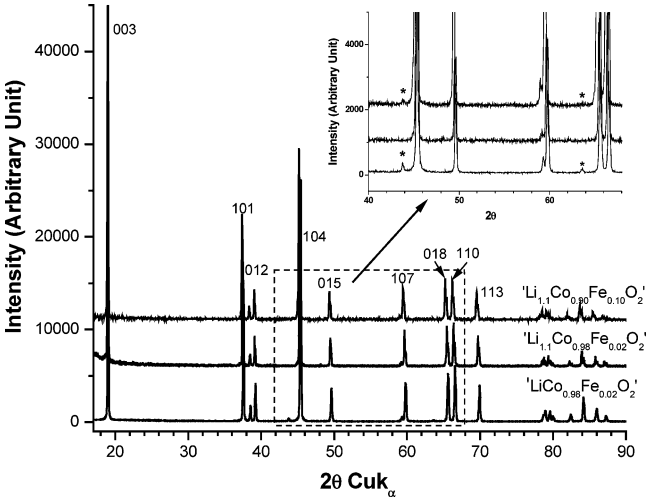

Figure 2. X-ray powder diffraction patterns of $LiCo_{0.98}Fe_{0.02}O_2$, "$Li_{1.1}Co_{0.98}Fe_{0.02}O_2$", and "$Li_{1.1}Co_{0.90}Fe_{0.10}O_2$" samples with Cu Kα radiation. Patterns in the 2θ range of 40−68° are enlarged on the top right, where small peaks corresponding to an impurity phase, α-$LiFeO_2$, are marked by asterisks.

and "$Li_{1.1}Co_{0.90}Fe_{0.10}O_2$" samples are shown in Figure 2. These samples appeared to be single-phase, and the diffraction peaks were indexed according to the hexagonal unit cell with space group $R\bar{3}m$. However, close examination revealed that a small amount of α-$LiFeO_2$ secondary phase with space group $Fm\bar{3}m$ (peaks marked with an asterisk) was found in the "$LiCo_{0.98}Fe_{0.02}O_2$" and "$Li_{1.1}Co_{0.90}Fe_{0.10}O_2$" patterns, as shown in the enlarged portion in the upper right corner in Figure 2. It should be pointed out that the intensity of the strongest α-$LiFeO_2$ peak is less than 0.8% of the (003) peak of the layered structure in the $LiCo_{0.98}Fe_{0.02}O_2$ sample. It is significant to note that iron substitution at 2 atom % in stoichiometric $LiCoO_2$ was not achieved in this study as α-$LiFeO_2$ impurity having space group $Fm\bar{3}m$ with Li^+ and Fe^{3+} ions randomly distributed on octahedral sites[10] was always found in the $LiCo_{0.98}Fe_{0.02}O_2$ samples prepared by the solid-state route at 900 °C through many attempts. The difficulty of iron substitution in stoichiometric $LiCoO_2$ can be explained by the fact that Fe^{3+} ions (0.645 Å) are much larger than Co^{3+} ions (0.54 Å) and Fe^{3+} ions cannot be accommodated in the CoO_6-type octahedral sites.[11] However, the presence of Fe^{3+} ions in the stoichiometric $LiCoO_2$ structure cannot be ruled out completely as the lattice parameters of the layered structure in the $LiCo_{0.98}Fe_{0.02}O_2$ sample are slightly greater than those of stoichiometric $LiCoO_2$ in this study and reported previously,[4] as shown in Table 1.

Iron substitution in lithium-overstoichiometric "$Li_{1.1}CoO_2$" samples was relatively facile and was limited to 10 atom % ($x = 0.10$) as the diffraction peaks (marked by an asterisk) of the α-$LiFeO_2$ secondary phase began to show in the "$Li_{1.1}Co_{0.90}Fe_{0.10}O_2$" sample. Iron-substituted lithium-overstoichiometric "$Li_{1.1}Co_{1-x}Fe_xO_2$" samples with $0.02 \le x \le 0.08$ were single-phase, having the layered structure with space group $R\bar{3}m$, as shown in Figure 3. All diffraction peaks were shown to shift to lower diffraction angles in 2θ as iron levels in the "$Li_{1.1}Co_{1-x}Fe_xO_2$" samples increased. Such a trend in the $(018)_{hex}$ and $(110)_{hex}$ peaks is shown clearly in the enlarged portion (upper right corner in Figure 3).

Table 1. Lattice Parameters of the Layered Structure for "$Li_{1.1}Co_{1-x}Fe_xO_2$" Samples with $0 \le x \le 0.08$ Refined by Profile Matching with the FullProf Computing Program[16]

x in $LiCo_{1-x}Fe_xO_2$	a_{hex} (Å)	c_{hex} (Å)
0 (Levasseur et al.[1])	2.81506(2)	14.0516(8)
0 (this work)	2.8137(8)	14.051(8)
0.02 (this work)[a]	2.818(1)	14.075(5)
x in $Li_{1.1}Co_{1-x}Fe_xO_2$	a_{hex} (Å)	c_{hex} (Å)
0 (Levasseur et al.[1])	2.81605(2)	14.0511(8)
0 (this work)	2.8157(7)	14.050(3)
0.02[57]	2.8167(8)	14.060(7)
0.04	2.8190(5)	14.075(5)
0.06[57]	2.8213(4)	14.090(4)
0.08	2.8233(4)	14.102(4)

[a] A small amount of α-$LiFeO_2$ secondary phase was found in the sample.

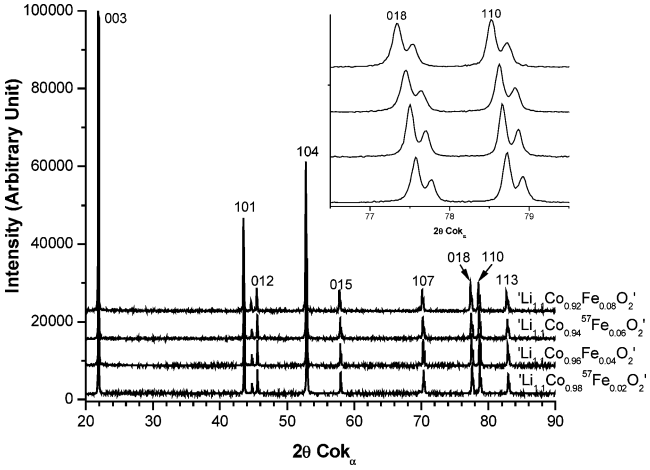

Figure 3. X-ray powder diffraction patterns of iron-substituted lithium-overstoichiometric "$Li_{1.1}Co_{1-x}Fe_xO_2$" samples having $0.02 \le x \le 0.08$ with Co Kα radiation, which were indexed to the layered structure with space group $R\bar{3}m$. The (018) and (110) peaks are enlarged in the top right corner of Figure 3, showing their shift and the doublet due to $K\alpha_2$ radiation.

It should be mentioned that considerably higher levels of iron substitution in $LiCoO_2$ were reported previously by Tabuchi et al. ($x = 0.25$)[10] and Kobayashi et al.[12] ($x = 0.30$) via hydrothermal synthesis, by Douakha et al.[13] ($x = 1.0$) via ion exchange from sodium precursors, and by Alcantara et al.[14] ($x = 0.30$) via solid-state synthesis at 800 °C. This discrepancy can be rationalized by the following: (1) in all these previous studies, lithium stoichiometry was not studied systematically and lithium overstoichiometry in the iron-substituted $LiCoO_2$ samples cannot be excluded, (2) different synthesis routes and temperatures might lead to metastable phases with different levels of iron substituted in $LiCoO_2$, and (3) significant mixing of Li^+ and Fe^{3+} ions in the layered structure was reported,[13,15] which suggests the formation of α-$LiFeO_2$-like domains.

(10) Tabuchi, M.; Ado, K.; Kobayashi, H.; Sakaebe, H.; Kageyama, H.; Masquelier, C.; Yonemura, M.; Hirano, A.; Kanno, R. *J. Mater. Chem.* **1999**, *9*, 199−204.
(11) Shannon, R. D.; Prewitt, C. T. *Acta Crystallogr.* **1969**, *B25*, 925.
(12) Kobayachi, H.; Shigemura, H.; Tabuchi, M.; Sakaebe, H.; Ado, K.; Kageyama, H.; Hirano, A.; Kanno, R.; Wakita, M.; Morimoto, S.; Nasu, S. *J. Electrochem. Soc.* **2000**, *147*, 960.
(13) Douakha, N.; Holzapfel, M.; Chappel, E.; Chouteau, G.; Croguennec, L.; Ott, A.; Ouladdiaf, B. *J. Solid State Chem.* **2002**, *163*, 406−411.
(14) Alcantara, R.; Jumas, J. C.; Lavela, P.; Olivier-Fourcade, J.; Pérez-Vicente, C.; Tirado, J. L. *J. Power Sources* **1999**, *81*−*82*, 547−553.

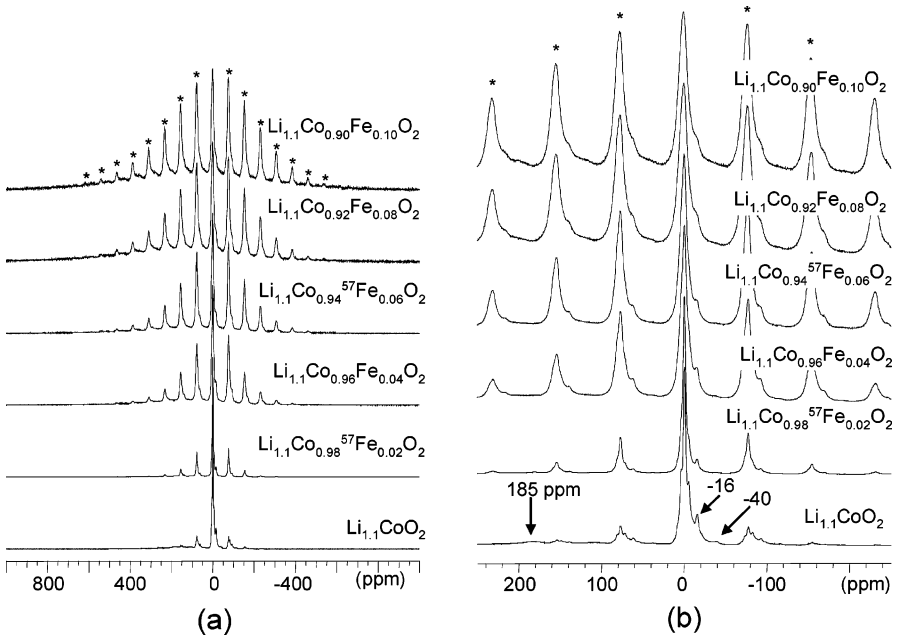

Figure 4. ^{7}Li MAS NMR spectra recorded for iron-substituted lithium-overstoichiometric samples in comparison to that of lithium-overstoichiometric $LiCoO_2$: (a) full scale, (b) expanded scale.

The hexagonal lattice parameters a_{hex} and c_{hex} of the layered structure for "$Li_{1.1}Co_{1-x}Fe_xO_2$" samples ($0.00 \leq x \leq 0.08$) were obtained by profile matching with the FullProf computing program,[16] and they were found to increase with iron substitution level x, as shown in Table 1. These refined lattice parameters were found in agreement with those of similar "$LiCo_{1-x}Fe_xO_2$" compounds reported in the literature.[10,13]

In the lithium-overstoichiometric samples, there are a large number of regular CoO_6 sites with a small fraction of square-pyramidal CoO_5 sites, namely, 8 atom % in the lithium-overstoichiometric "$Li_{1.1}CoO_2$" sample with an oxygen vacancy concentration of $t = 0.04$ as reported previously.[6] Provided that substituted iron ions were in a high-spin 3+ state, Fe^{3+} ions (0.645 Å) are much larger than Co^{3+} ions (0.54 Å)[11] and reported Fe−O bond length values[15] (2.081 Å in α-$LiFeO_2$ with space group $Fm\bar{3}m$ and 2.029 Å in $LiFeO_2$ with space group $R\bar{3}m$) in the octahedral environment are much larger than the Co−O bond length in layered $LiCoO_2$ (1.924 Å). As Fe^{3+} ions cannot reside in regular octahedral sites of the $LiCoO_2$ structure but they can be substituted for Co^{3+} in the Li-overstoichiometric samples, we speculate that Fe^{3+} ions preferentially reside in square-pyramidal MO_5 sites upon substitution of Co^{3+}. The presence of an oxygen vacancy in such a defect site decreases the constraints around the large Fe^{3+} ions in the slab relative to those of the octahedral environment in stoichiometric $LiCoO_2$.

^{7}Li NMR. Figure 4a shows the ^{7}Li MAS NMR spectra recorded for iron-substituted lithium-overstoichiometric samples in comparison to that of lithium-overstoichiometric "$Li_{1.1}CoO_2$". The unsubstituted lithium-overstoichiometric material exhibits the additional signals vs stoichiometric $LiCoO_2$ that we discussed in previous papers.[4,6] Our previous studies in nickel-substituted $LiCoO_2$[17] showed that signals at 110 ppm and at −15 and −30 ppm were associated with interactions between Li ions and e_g electron spins from Ni^{3+} with 180° and 90° Ni^{3+}−O−Li configurations, respectively. Therefore, it is believed that the main additional signals observed in Fe^{3+}-free and Fe^{3+}-substituted lithium-overstoichiometric "$Li_{1.1}CoO_2$" at +185 ppm and at −16 and −40 ppm result from interactions with the d_{z^2} orbital of $Co^{3+(IS)}$ that carries a spin, as shown in Figure 4b.[6] However, some electron spin density can be transferred to other lithium ions by alternative pathways as the d_{xy} orbital of $Co^{3+(IS)}$ also carries a spin and points toward Li^+ ions. A direct transfer of electron spin density can also be envisaged from the d_{z^2} orbital lobe facing the oxygen vacancy, although the Li^+ ion is rather far. Therefore, it is speculated that additional NMR signals observed in these samples (in particular the shoulders at +4 and −6 ppm) might be associated with interactions with Li^+ ions in combinations of these various configurations. However, due to the complexity of the situation, a full assignment of these signals could not be completed in this study.

Upon iron substitution, a clear feature in Figure 4 is general broadening of the spectra, which includes broadening of the individual spinning sidebands and an increase of the number of spinning sidebands. This is most probably a result of a very strong through-space dipolar interaction exerted by the electron spins of Fe^{3+} on the Li^+ ions. We will return to this discussion in the following section.

Another important observation for $x = 0.02$ is a relative decrease, in comparison to that of the "$Li_{1.1}CoO_2$" sample, of the magnitude of the extra signals, which were considered to be characteristic of Li^+ ions next to intermediate-spin Co^{3+} ions in the square-pyramidal sites.[6] This is consistent with

(15) Tabuchi, M.; Ado, K.; Kobayashi, H.; Matsubara, I.; Kageyama, H.; Wakita, M.; Tsutsui, S.; Nasu, S.; Takeda, Y.; Masquelier, C.; Hirano, A.; Kanno, R. *J. Solid State Chem.* **1998**, *141*, 554−561.
(16) Rodriguez-Carvajal, J. *Physica B* **1993**, *192*, 55−69.
(17) Carlier, D.; Ménétrier, M.; Delmas, C. *J. Mater. Chem.* **2001**, *11*, 597−603.

the assumption that Fe^{3+} will occupy these sites by replacing a part of the intermediate-spin Co^{3+} ions associated with the proposed defect model. For higher values of *x*, however, the correlation between the relative magnitude of the extra signal vs Fe^{3+} content is not straightforward due to the broadening of the lines for *x* higher than 0.04. The anisotropy of the various signals (and therefore their relative magnitude in the isotropic signal) can be different and the global anisotropy changes drastically, which makes the estimation of the relative amount of these signals rather difficult. In addition, the extent of lithium overstoichiometry of different samples prepared in this study is dependent on the preparation details such as the exact heat-treatment duration, the oxygen flow rate, and the surface of the samples exposed to flowing oxygen per unit weight during heat treatments. Therefore, the magnitude of extra signals and the Fe^{3+} level cannot be correlated quantitatively in this study. The important fact is that these extra signals did not disappear completely upon iron substitution, even in the $x = 0.10$ sample with a small amount of α-$LiFeO_2$ impurity phase found by X-ray diffraction (Figure 2). The presence of these signals in the highly Fe^{3+} substituted samples suggests that some intermediate-spin Co^{3+} ions are still present in the square pyramids associated with oxygen vacancies for the high values of *x*, which implies that not all Fe^{3+} ions were accommodated in the square-based pyramidal defect sites for $x = 0.08$. This is most probably due to the difficulty of obtaining the thermodynamically favorable Fe/Co distribution during the synthesis, which may require prolonged annealing durations.

It should, however, be noted that no extra signal was observed by NMR upon iron substitution in lithium-overstoichiometric samples, even in the $x = 0.10$ sample where α-$LiFeO_2$ was detected by X-ray powder diffraction. This is consistent with the fact that, in layered $LiFeO_2$ with space group $R\bar{3}m$, Fe^{3+} in an octahedral environment is high-spin d^5, and the electron spins thus exert such strong interactions on the neighboring Li^+ that they can hardly be observed by NMR.[18] Some of the iron in the samples with high values of *x* may form nanodomains of α-$LiFeO_2$, which is based on the same oxygen packing but has a cation arrangement different from that of $LiCoO_2$. The volume fraction and/or size of such domains would be too small to be detected by X-ray powder diffraction for $x \leq 0.08$, while it is high enough for X-ray diffraction detection at $x = 0.10$, where more iron is present than the number of available defect sites and NMR shows that some IS Co^{3+} ions in the square-based pyramids remain. In any case, octahedral Li^+ ions sharing edges with such octahedral, high-spin Fe^{3+} ions cannot be observable by NMR, but the presence of high-spin Fe^{3+} leads to strong diffuse dipolar broadening as substituted Fe^{3+} levels increase, as shown in Figure 4.

It should also be mentioned that the presence of Fe^{3+} ions in the square-based pyramid sites should exert additional hyperfine interactions on the adjacent Li^+ ions, in a manner depending on the actual spin state of iron. In our ^7Li MAS NMR spectra, signals associated with the Li^+ ions adjacent to Fe^{3+} ions in the square-based pyramids were not identified,

(18) Carlier, D. Ph.D Dissertation, Université Bordeaux I, 2001.

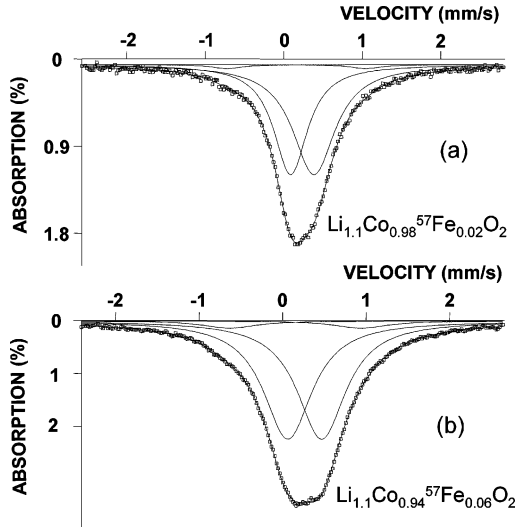

Figure 5. Mössbauer spectra of (a) "$Li_{1.1}Co_{0.98}{}^{57}Fe_{0.02}O_2$" and (b) "$Li_{1.1}Co_{0.94}{}^{57}Fe_{0.06}O_2$" samples collected at room temperature, which were fitted using Lorentzian lines.

Table 2. Isomer Shifts and Quadrupole Splittings of the Iron Environments in the "$Li_{1.1}Co_{0.98}{}^{57}Fe_{0.02}O_2$" and "$Li_{1.1}Co_{0.94}{}^{57}Fe_{0.06}O_2$" Samples Synthesized Using $^{57}Fe_2O_3$, Obtained by Spectrum Fitting Using Two Lorentzian Lines (See Figure 5)

	δ (mm·s^{-1})	Δ (mm·s^{-1})	Γ (mm·s^{-1})	%
$Li_{1.1}Co_{0.98}{}^{57}Fe_{0.02}O_2$				
1	0.249(9)	0.298(9)	0.58(2)	97
2	0.17(10)	1.77(10)	0.50(10)	3
$Li_{1.1}Co_{0.94}{}^{57}Fe_{0.06}O_2$				
1	0.275(3)	0.406(2)	0.70(10)	94
2	0.16(5)	1.57(10)	0.80	6

which is consistent with the hypothesis that Fe^{3+} ions retain a high-spin (HS) configuration in the square-based pyramid.[19,20] If, however, Fe^{3+} ions in the square-based pyramids were to be IS $[(d_{xz}d_{yz})^3d_{xy}{}^1d_{z^2}{}^1]$, they might lead to the nearby Li ions being partly NMR observable, since the additional $d_{xz}d_{yz}$ single electron present should make part of such Li ions unobservable. It can therefore not be totally excluded that such a situation could lead to weak signals obscured by the resonances assigned to interaction with IS Co^{3+} ions. Support for HS Fe^{3+} in iron-substituted lithium-overstoichiometric samples will be discussed in detail in the following section.

Mössbauer Spectroscopy. ^{57}Fe-enriched samples with nominal compositions of "$Li_{1.1}Co_{0.98}{}^{57}Fe_{0.02}O_2$" and "$Li_{1.1}Co_{0.94}{}^{57}Fe_{0.06}O_2$" were characterized by Mössbauer spectroscopy at room temperature. The spectra of these two samples are shown in parts a and b, respectively, of Figure 5. They exhibit asymmetrical peaks that can be decomposed into Lorentzian lines in the first treatment assigned to two quadrupolar doublets for each compound, having one component (with the larger quadrupolar splitting value) in very small proportion. The isomer shifts, quadrupole splittings, line widths, and percentages of different iron environments obtained in this treatment are listed in Table 2.

(19) Buffat, B.; Demazeau, G.; Pouchard, M.; Hagenmuller, P. *Proc.*—Indian Acad. Sci., Chem. Sci. **1984**, *93*, 313−320.
(20) Demazeau, G.; Buffat, B.; Pouchard, M.; Hagenmuller, P. *J. Solid State Chem.* **1982**, *45*, 88−92.

Table 3. Isomer Shifts and Quadrupole Splittings of the Fe Environments in the "$Li_{1.1}Co_{0.98}{}^{57}Fe_{0.02}O_2$" and "$Li_{1.1}Co_{0.94}{}^{57}Fe_{0.06}O_2$" Samples Synthesized Using $^{57}Fe_2O_3$, Obtained by Spectrum Fitting Using Distributions of Quadrupole Doublets (See Figure 6)[a]

	δ (mm·s^{-1})	Γ (mm·s^{-1})	Δ_m* (mm·s^{-1})	%*
$Li_{1.1}Co_{0.98}{}^{57}Fe_{0.02}O_2$				
DIS 1	0.249	0.35	0.4	97
DIS 2	0.17	0.35	1.6	3
$Li_{1.1}Co_{0.94}{}^{57}Fe_{0.06}O_2$				
DIS 1	0.275	0.35	0.3-0.6	95
DIS 2	0.16	0.35	1.0	5

[a] The minority component for each material is not considered in the data analysis (see the text).

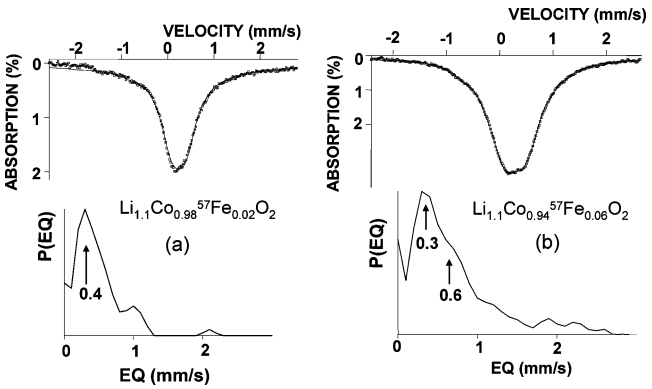

Figure 6. Mössbauer spectra of (a) "$Li_{1.1}Co_{0.98}{}^{57}Fe_{0.02}O_2$" and (b) "$Li_{1.1}Co_{0.94}{}^{57}Fe_{0.06}O_2$" samples collected at room temperature, which were fitted using two distributions of quadrupole doublets, with the corresponding distribution profile for the majority component.

As the first treatment led to rather broad lines whose quadrupolar splitting values (considerably larger than 0.35 mm·s^{-1}) may not be meaningful, the spectra were then fitted in the second calculation to two distributions of quadrupole doublets. In the second treatment, the relative probability and quadrupolar splitting were set as free parameters, having their isomer shift fixed to the value determined in the first treatment and their line width fixed to 0.35 mm·s^{-1}. The corresponding isomer shift and quadrupole splitting values obtained from the second computation are tabulated in Table 3. Like in the first treatment, one dominant iron environment (distribution) (>94%) was found for both samples. Considering the experimental uncertainty of the Mössbauer parameters of the minority distributions and their relative magnitude, the minor iron environments are not discussed in this paper.

For the 2 atom % iron-substituted sample, the dominant distribution was relatively narrow and led to a single value of quadrupole splitting, while a somewhat broader distribution was found for the 6 atom % sample, as shown in Figure 6. It should be noted that the isomer shift, $\delta = 0.249$ mm·s^{-1}, in the "$Li_{1.1}Co_{0.98}{}^{57}Fe_{0.02}O_2$" sample, is considerably smaller than the values of major iron environments (octahedral, high-spin Fe^{3+}) in similar layered iron-substituted cobalt and nickel oxide samples reported previously by Prado et al. ($\delta = 0.33$ mm·s^{-1}).[21] In addition, it was found that this isomer shift is significantly lower than typical isomer shifts (with an average $\delta = 0.37$ mm·s^{-1}) for octahedral FeO_6 environments surveyed in the literature,[7,22,23] as shown in Table 4. As isomer shifts decrease with decreasing iron coordination for a given oxidation state of iron and a given ligand shown in Table 4, the low isomer shift observed in the "$Li_{1.1}Co_{0.98}{}^{57}Fe_{0.02}O_2$" sample is consistent with the hypothesis that most $^{57}Fe^{3+}$ ions reside in the square-pyramidal FeO_5 sites instead of FeO_6 sites. We believe that oxygen positions in FeO_5 sites are not significantly altered; therefore, FeO_5 trigonal-bipyramidal sites with isomer shifts similar to those of square-pyramidal sites are not considered in this study.

Table 4. Experimental Reported Isomer Shifts of Oxides Containing Fe^{3+} in Octahedral FeO_6, FeO_5 Square-Pyramidal, FeO_5 Trigonal-Bipyramidal, and FeO_4 Tetrahedral Coordination at Room Temperature Compiled from Previous Studies[7,22,23]

iron coordination	experimentally obsd ranges for isomer shifts (mm·s^{-1})
octahedral FeO_6	0.41−0.30
FeO_5 square pyramid	0.24−0.31
FeO_5 trigonal bipyramid	0.34−0.22
tetrahedral FeO_4	0.24−0.11

A difference with literature data for iron in the square-based pyramid environment lies in the quadrupole splitting value. In such a configuration, Fe is usually considered to be intermediate-spin $[(d_{xz}d_{yz})^3d_{xy}{}^1d_{z^2}{}^1]$; such a nonspherical distribution of the electrons on the d orbitals of iron leads to a strong electrical field gradient (EFG) and, consequently, to large quadrupole splitting values (1.65 mm·s^{-1} for ^{57}Fe-doped $Sr_2Co_2O_5$,[23] 1.8 mm·s^{-1} for ^{57}Fe $La_2Li_{0.5}Co_{0.5}O_4$,[24,25] and 1.84 mm·s^{-1} for ^{57}Fe-doped $La_2Li_{0.5}Cu_{0.5}O_4$[26]). The much lower quadrupole splitting value observed (0.4 mm·s^{-1}) for "$Li_{1.1}Co_{0.98}{}^{57}Fe_{0.02}O_2$" therefore suggests that Fe^{3+} has an HS configuration $[(d_{xz}d_{yz})^2d_{xy}{}^1d_{z^2}{}^1d_{x^2-y^2}{}^1]$ with an equal occupancy of the five d orbitals. The contribution of the d electrons to the EFG is therefore null, and the weaker effect of oxygen ion distribution only remains. As a matter of fact, the observed value is slightly larger than that for the usual HS octahedral iron (0.35 mm·s^{-1} for $Li_{0.97}(Ni_{0.70}Fe_{0.15}Co_{0.15})_{1.03}O_2$[27]), which is in agreement with a distorted oxygen environment such as a square-based pyramid. This assumption of Fe^{3+} being in an HS state in "$Li_{1.1}Co_{0.98}{}^{57}Fe_{0.02}O_2$" is also in agreement with the fact that no Li NMR signal related to the presence of iron could be detected.

As Fe substitution levels increase from $x = 0.02$ to $x = 0.06$, we note that the isomer shift of major quadrupole signals was found to rise, although the isomer shift of "$Li_{1.1}Co_{0.94}{}^{57}Fe_{0.06}O_2$" is still lower than the average expected for octahedral FeO_6 coordination.

In addition to the rise of isomer shift upon iron substitution, the quadrupole splitting distribution was found to be different

(21) Prado, G.; Fournès, L.; Delmas, C. *J. Solid State Chem.* **2001**, *159*, 103.
(22) Doumerc, J. P.; Coutanceau, M.; Fournes, L.; Grenier, J. C.; Pouchard, M.; Wattiaux, A. *C. R. Acad. Sci., Ser. IIc: Chim.* **1999**, *2*, 637−643.
(23) Grenier, J. C.; Fournes, L.; Pouchard, M.; Hagenmuller, P. *Mater. Res. Bull.* **1986**, *21*, 441−449.
(24) Demazeau, G.; Pouchard, M.; Colombet, J. F.; Grenier, J. C.; Thomas, M.; Fournès, L.; Soubeyroux, J. L.; Hagenmuller, P. *C. R. Acad. Sci. Paris* **1979**, *289C*, 231−234.
(25) Demazeau, G.; Pouchard, M.; Thomas, M.; Colombet, J. F.; Grenier, J. C.; Fournes, L.; Soubeyroux, J. L.; Hagenmuller, P. *Mater. Res. Bull.* **1980**, *15*, 451−459.
(26) Buffat, B.; Demazeau, G.; Pouchard, M.; Hagenmuller, P. *Mater. Res. Bull.* **1983**, *18*, 1153−1158.
(27) Prado, G.; Suard, E.; Fournès, L.; Delmas, C. *J. Mater. Chem.* **2000**, *10*, 2553.

for the two samples. The quadrupole splitting of $Li_{1.1}Co_{0.98}Fe_{0.02}O_2$ exhibits a single major value ($\Delta = 0.4$ mm·s^{-1}) as discussed above, whereas the "$Li_{1.1}Co_{0.94}{}^{57}Fe_{0.06}O_2$" material exhibits a broad distribution that was decomposed to two main quadrupole splitting values, close to 0.3 and 0.6 mm·s^{-1}, which suggested the presence of Fe^{3+} in two different environments. Considering the resolution of the spectra, it is not possible to ascertain whether these two environments could correspond to different isomer shift values or not. Therefore, the two types of Fe^{3+} environments in the 6 atom % substituted sample could be related to different defect chemistries, namely, one or two Fe^{3+} ions per defect site or Fe^{3+} ions in octahedral sites of α-$LiFeO_2$-type domains as suggested from the NMR results and the fact that the (global) isomer shift is higher than for the "$Li_{1.1}Co_{0.98}{}^{57}Fe_{0.02}O_2$" sample.

Conclusion

The present NMR and Mössbauer characterization of iron-substituted lithium-overstoichiometric "$Li_{1.1}CoO_2$" provides further support to the defect model that we proposed earlier, namely, the presence of oxygen vacancies resulting from excess lithium in substitution for cobalt, leading to intermediate-spin Co^{3+} ions in square-based pyramids.

First, Fe^{3+} cannot substitute Co^{3+} in lithium-stoichiometric $LiCoO_2$ using direct high-temperature synthesis as Fe^{3+} ions are considerably larger than Co^{3+} ions.

Second, some Co^{3+} in square-based pyramids can be replaced by Fe^{3+} in lithium-overstoichiometric "$Li_{1.1}CoO_2$". At low levels of iron substitution (2 atom %), the presence of an Fe^{3+} environment with peculiar Mössbauer parameters (isomer shift 0.25 mm·s^{-1}, quadrupole splitting 0.4 mm·s^{-1}) is consistent with HS Fe^{3+} in square-based pyramidal sites. At high levels of iron substitution (6 atom %), it is hypothesized that some Fe^{3+} ions would partially mix with Li^+ ions to form α-$LiFeO_2$-type domains in regular octahedral sites (HS octahedral Fe^{3+}) rather than occupy all the available square-pyramidal $Co^{3+(IS)}O_5$ defect sites.

Acknowledgment. We thank Région Aquitaine for financial support and Catherine Denage for her technical assistance. Y.S.-H. acknowledges the support of NSF International Research Fellow Award INT-0000429 and a visiting professorship from the Université Bordeaux I.

CM0504384